ELSEVIER

Catalysis Today 65 (2001) 249–256

CATALYSIS TODAY

www.elsevier.com/locate/cattod

Aromatic reduction properties of molybdenum sulfide clusters in HY zeolite

Pierre Leyrit [a], Tivadar Cseri [a,*], Nathalie Marchal [a], John Lynch [b], Slavik Kasztelan [a]

[a] Institut Français du Pétrole, Kinetics and Catalysis Division, 1-4 avenue de Bois Préau, F-92852 Rueil-Malmaison, France
[b] Physics and Analysis Division, 1-4 avenue de Bois Préau, F-92852 Rueil-Malmaison, France

Abstract

Molybdenum sulfide catalysts supported on an HY zeolite at various Mo contents were studied. Catalysts were prepared by incipient wetness impregnation with ammonium heptamolybdate solution and calcined without drying. Their reactivity has been evaluated in toluene hydrogenation under typical hydrotreating conditions. Compared to alumina supported catalysts, zeolite supported Mo catalysts are extremely active for aromatics hydrogenation. At low molybdenum loading, molybdenum sulfide phases inside the zeolite show a particularly high intrinsic activity. This activity can be attributed to molybdenum sulfide clusters differing from MoS_2 slabs. © 2001 Elsevier Science B.V. All rights reserved.

Keywords: Molybdenum sulfide; Catalysts; Zeolite; Hydrogenation

1. Introduction

New regulations concerning sulfur and aromatics content of gasoil have recently stimulated studies on catalysts for the deep hydrogenation or aromatics saturation of gasoil [1]. In this respect, zeolites are good candidates as supports for the active phase because they provide a highly specific surface likely to enhance active phase dispersion and therefore catalytic activity [2]. Moreover, zeolites are promising supports for hydrotreatment catalysts because such catalysts would combine a hydrogenation function provided by the sulfide phase (Mo, Co, Ni) with the acidic function of the zeolite. Some recent studies [3–8] have already shown that zeolite supported metal sulfides are highly active in hydrodesulfurization or hydrogenation reactions and that acidity of the zeolite promotes their activity. According to Welters [3,9] this beneficial effect could be explained either by a better absorption of the reactants in zeolite pores or by an acceleration of the rate determining step of the reaction, or by changes in the catalytic properties of the metal sulfide phase due to electron transfer. This latter hypothesis was confirmed by Breysse [7] on the basis of previous studies on metallic catalysts [10].

Molybdenum is at present difficult to disperse on zeolite by convenient methods. Molybdenum deposition by adsorption of a carbonyl complex ($Mo(CO)_6$) from a vapor phase or from a solution seems to lead to good results but this method is delicate in use [11–13]. Another efficient method would be ion exchange but cationic salts of Mo are scarce and not stable [14]. Therefore, the most often used method is incipient wetness impregnation of ammonium heptamolybdate solution even if this salt leads to an anionic $Mo_7O_{24}^{6-}$ form whose size makes it unable to penetrate zeolite cavities [4]. Moreover, this method is known to favor loss of zeolite crystallinity [15–17] and very low dispersion of Mo [18,19]. An

---

[*] Corresponding author. Fax: +33-147-52-6055.
E-mail address: tivadar.cseri@ifp.fr (T. Cseri).

PII: S0920-5861(00)00594-0

efficient method to prepare highly dispersed Mo zeolite supported catalysts would consist in calcining these catalysts in humid air. Indeed water seems to favor the formation of volatile species ($MoO_2(OH)_2$) that can diffuse into zeolite cavities [20–22].

The objective of this study is to prepare highly dispersed Mo/HY catalysts by the incipient wetness impregnation method at various Mo loadings and to determine their activity in toluene hydrogenation in the presence of H_2S. The catalytic activities will be compared with those of conventional Mo, CoMo and NiMo catalysts supported on γ-alumina.

2. Experimental

2.1. Catalyst preparation

Molybdenum based catalysts at various metal loadings (1.6, 5.1, 8.3 wt.% of Mo) were prepared on dealuminated zeolite HY ($Si/Al = 19$) powder by incipient wetness impregnation with ammonium heptamolybdate solution. Catalysts were then calcined (500°C, 2 h, in air flow) without prior drying to favor the formation of ($MoO_2(OH)_2$) species and to facilitate molybdenum diffusion into the zeolite cavities [23]. Finally, they were pelleted (4 mm diameter) for catalytic tests.

2.2. Catalytic measurements

Hydrogenation of toluene was performed in a fixed-bed reactor in continuous flow at 300°C under 6 MPa total pressure over sulfided catalysts. Dimethyldisulfide was added to the feed in order to maintain a high H_2S partial pressure and *n*-hexane was used as solvent. LHSV was $1\,h^{-1}$ and partial pressures were 5.17 MPa for hydrogen, 0.13 MPa for toluene, 0.56 MPa for *n*-hexane and 0.07 MPa for H_2S.

2.3. Catalyst characterization

All characterization analyzes were performed on catalysts previously sulfided with a H_2/H_2S mixture (15% mol H_2S) at 400°C, 2 h, heating rate 5°C/min. After evacuation at 2×10^{-5} mbar, the samples were transferred immediately to sealed cells to avoid any contact with air and oxidation.

The molybdenum content was determined by X-ray fluorescence and the sulfur content by combustion.

Ultramicrotome sections of the samples were studied by high resolution transmission electron microscopy (HRTEM) and scanning transmission electron microscopy for local analysis (STEM-EDX).

Temperature programmed reduction (TPR) experiments were carried out using an Xsorb® automatic solid catalysts characterization unit from GIRA coupled with gas chromatography using a flame photonic detector (FPD). With this coupled system, during TPR, we detect simultaneously the H_2 consumption (TCD) and the H_2S production (FPD) as a function of temperature. All TPR experiments were realized in the same conditions on 100 mg of catalysts.

Extended X-ray absorption fine structure (EXAFS) experiments were carried out at LURE (Orsay) in transmission mode at the Mo K-edge. EXAFS data were taken in the transmission mode through a double crystal monochromator (Si 1 1 1) using two ion chambers as detectors. X-ray absorption specta were taken in the 19 000–20 900 eV range. The Mo K-edge EXAFS region for Mo catalysts were analyzed using a standard data analysis procedure (SIMPLEX software package [24]). The EXAFS spectra was first transformed from k space (k^3 hamming windows 3.5, 5.5, 11, 13 $Å^{-1}$) to r space to obtain the radial distribution function (RDF). The EXAFS spectrum for one or several coordination shells was isolated by inverse Fourier transform of the RDF over the appropriate region and fitted using the single scattering EXAFS equation. For all catalysts the Debye–Waller factor (established on a reference sample) was maintained constant and respectively equal for Mo–O, Mo–S and Mo–Mo shells to 60×10^{-3}, 60×10^{-3} and 70×10^{-3} $Å^2$.

3. Results and discussion

3.1. Catalytic activities

In our experimental conditions, toluene hydrogenation produces methylcyclohexane. Because of the supports acidity methylcyclohexane can however be further isomerized and cracked. Aromatics (xylenes) formed by disproportionation reactions are also observed in minor amounts. These products are partially hydrogenated, isomerized and cracked. Cracking

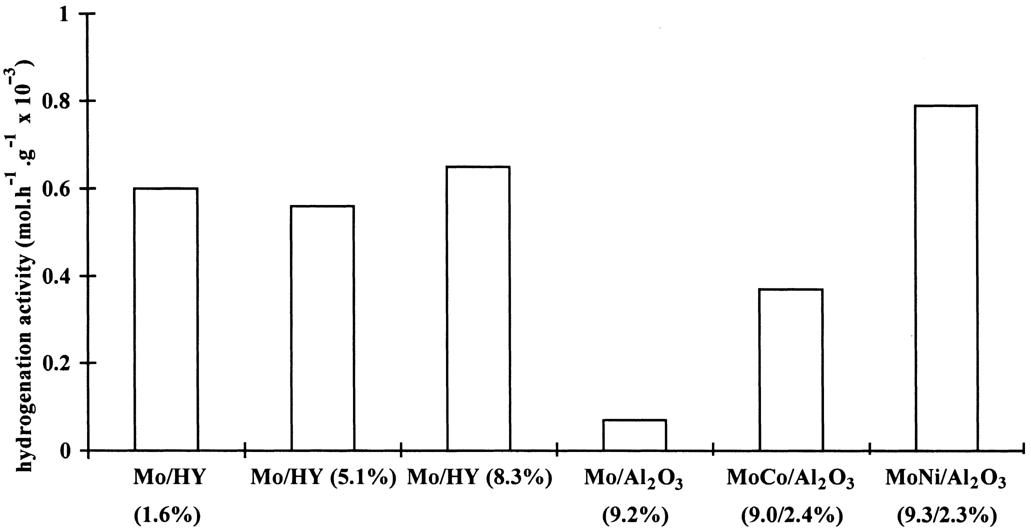

Fig. 1. Hydrogenation activity per gram of catalyst.

reactions do not occur on aromatic molecules. In consequence all non-aromatic products that are detected after the catalytic reaction (liquid and gas compounds) come from an aromatic hydrogenation reaction.

Global activity in hydrogenation must then be calculated including all products having a hydrogenation step in their reaction path. These activities (assuming a first order reaction) were calculated in carbon equivalent and further expressed in moles of toluene converted per hour and per gram of catalyst (Fig. 1) or per mole of molybdenum (Fig. 2). They are compared with those obtained from conventional Mo, CoMo and NiMo catalysts supported on γ-alumina.

The activities of Mo/HY catalysts calculated per gram of catalyst are very similar whatever be the Mo content as shown in Fig. 1. High activities are reached with small Mo content and additional Mo does not seem to contribute to activity enhancement.

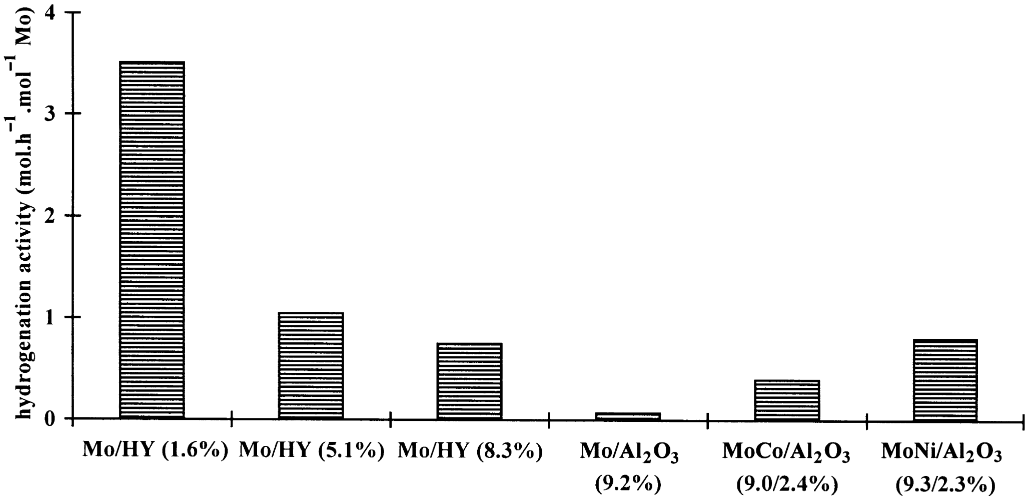

Fig. 2. Hydrogenation activity per mole of molybdenum.

At equivalent loading (about 9 wt.% Mo), molybdenum sulfide is close to 10 times more active when supported on zeolite HY than on alumina. Moreover, all Mo/HY catalysts show hydrogenation activity higher than $CoMo/Al_2O_3$ and close to $NiMo/Al_2O_3$.

When expressed per mole of molybdenum, the hydrogenation activity of Mo/HY catalysts strongly decreases when Mo loading increases. The intrinsic activity of Mo/HY (1.6%) is remarkably high compared to the other Mo/HY catalysts and to conventional alumina supported catalysts.

Our catalytic results could suggest that:

- At low Mo loading, molybdenum is extremely dispersed into zeolite HY probably because of the particular preparation of the catalysts.
- The sulfided phase is highly active. This is likely to be due to its proximity to acid sites.

Recent studies have already shown that zeolite supported Mo catalysts could demonstrate higher activities than conventional Mo/Al_2O_3 catalysts [3–5,9] due to the acidity support. However, most of these studies deal with high Mo loading catalysts, and only [25] mention high Mo specific activity for HDS of gasoil at low Mo content.

3.2. Catalyst characterization

3.2.1. Sulfur content

The S/Mo ratio of the active phase was obtained by subtracting the amount of sulfur measured on pure “sulfided” HY zeolite (corresponding to the estimated sulfur deposited on the support) from the amount of sulfur measured on the Mo/HY catalysts. The sulfidation degrees obtained by comparison with those of theoretical S/Mo ratio of 2 (MoS_2 phase) are presented in Table 1.

S/Mo atomic ratio decreases from 2.09 to 1.24 when Mo loading increases from 1.6 to 8.3 wt.% indicating that Mo is likely to be fully sulfided at low Mo content and only partially at higher Mo loading (from 100 to 62%).

Table 1
S/Mo atomic ratio and sulfidation degree of Mo/HY catalysts

Catalysts	Mo (wt.%)	S/Mo	Sulfidation degree (%)
Mo/HY	1.6	2.09	100
Mo/HY	5.1	1.45	72
Mo/HY	8.3	1.24	62

These results show a trend similar to other studies reported in the literature [26–28]. However, we can note that even at high Mo loading the sulfidation degree is still good compared to other reported results [17,29].

The catalytic activity shown in Fig. 2 can be corrected by these sulfidation degrees. However, this drop in sulfidation degree as a function of Mo loading does not entirely explain the loss of Mo intrinsic hydrogenation activity with increasing Mo content. For a better understanding of the catalytic phenomena, complementary characterizations of sulfided catalysts were performed.

3.3. TEM–STEM–EDX analysis

TEM micrograph of Mo/HY catalysts at 1.6, 5.1 and 8.3 wt.% Mo show the presence of the Mo/HY catalysts in three distinct forms. The distribution of molybdenum sulfide species is summarized in Table 2.

Small aggregates (7–25 Å) are detected on all samples. EDX analysis has demonstrated that they are composed of sulfided Mo. MoS_2 slabs one to two sheets in height and 10–60 Å in length were present only on samples with higher Mo loading (5.1 and 8.3%). On the highest loading catalyst, large particles (>100 Å) were also observed corresponding to unsulfided MoO_x phases. Some of the latter ones are surrounded by MoS_2 slabs and look like inorganic fullerenes recently described [30,31].

On zeolite ultramicrotome sections, no slabs or aggregates were observed on the external surface of HY crystals but some particles were detected. Some slabs are also present around the mesopore surfaces. The

Table 2
Molybdenum sulfide species observed on sulfided Mo/HY catalysts

MoS_x species	Mo loading of Mo/HY catalysts (wt.%)		
	Mo (1.6%)	Mo (5.1%)	Mo (8.3%)
Small aggregates (7–25 Å)	+	+	+
MoS_2 slabs (10–60 Å)		+	+
Large particles (>100 Å)			+

major part of slabs and small particles are homogeneously distributed on the zeolite framework. It is not possible to locate these particles precisely and we cannot determine by this technique if the small particles are inside the zeolite cages (in TEM sections are visualized in projection). However, it seems that the particles are uniformly distributed within the zeolite grains.

The distribution of Mo species on HY zeolite is far different from that on alumina supported catalysts where only MoS_2 slabs are observed by TEM. The evolution of Mo species distribution with Mo content (appearance of slabs and large particles) can be explained by the decrease in the Mo dispersion. Several authors have indeed observed the formation on zeolite supported catalysts of large particles with increasing Mo content [5,27,28] but in our case, we do not observe any highly stacked slabs at the external surface of the zeolite.

In comparison with the catalytic activity results (expressed per gram of catalyst), we can suppose that small aggregates could be the highly active species. MoS_2 slabs and large particles observed at higher Mo loading would have only a very small contribution to the total catalytic activity.

3.4. EXAFS experiments

Table 3
Results of EXAFS fitting for Mo catalysts

Catalysts	Mo–O		Mo–S		Mo–Mo	
	N^a	R^b	N	R	N	R
MoS_2	–	–	6	2.41	6	3.16
Mo/Al_2O_3 (12%)	0.8	1.62	5.4	2.38	4.3	3.18
Mo/HY (1.6%)	0.4	1.77	3.8	2.40	1.7	3.11
Mo/HY (5.1%)	0.3	1.75	3.6	2.40	1.9	3.13
Mo/HY (8.3%)	0.3	1.75	3.1	2.40	1.4	3.11

[a] Coordination number.
[b] Coordination length (Å).

Table 3 presents the results of EXAFS fitting of data from the Mo/HY catalysts compared to MoS_2 theoretical data [32] and a conventional Mo/Al_2O_3 catalyst. The Fourier transform moduli of EXAFS are shown in Fig. 3.

On all catalysts Mo–S and Mo–Mo shells are detected but a Mo–O coordination is also observed. The latter is, according to de Boer [33], attributed to a Mo=O coordination corresponding to the presence of a residual oxide phase (MoO_2–MoO_3). However, in the case of Mo/HY catalysts, the number of O neighbors is relatively small (from 0.3 to 0.4) and independent of the Mo content. Mo/HY catalysts have similar characteristics: the Mo–S coordination (at 2.40 Å) decreases from 3.8 to 3.1 when the Mo content increases. The Mo–Mo coordination is between 1.4 and 1.9 at distances between 3.11 and 3.13 Å. These coordination numbers are very low compared to those

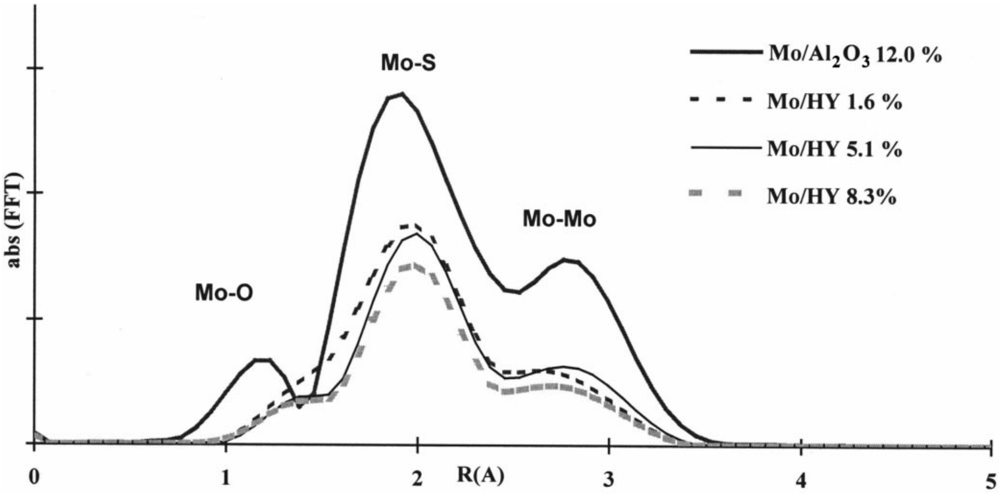

Fig. 3. Fourier transform moduli of EXAFS for Mo catalysts.

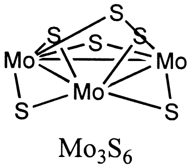

Scheme 1. Mo_3S_6 structure.

of a conventional Mo/Al_2O_3 catalyst (Mo–S = 5.4 at 2.38 Å and Mo–Mo = 4.3 at 3.18 Å).

Although EXAFS is known to underestimate Mo–Mo coordination in these systems, due to high structural disorder [34], these very low coordination numbers suggest the presence in the HY catalysts of small MoS_x clusters that do not exist on alumina. The decrease in Mo–Mo distances (from 3.18 Å to around 3.13 Å) may also be characteristic of the presence of small clusters of Mo atoms [35].

These particles could be of a structure similar to Mo_3S_6 (S/Mo ratio of 2) presented on Scheme 1, whose Mo–Mo coordination is 2 and Mo–S coordination is 4. According to Diemann et al., these clusters involve coordinately unsaturated molybdenum atoms and are expected to exhibit high reactivity [36].

3.5. TPR studies

Figs. 4 and 5 show the simultaneously measured H_2 consumption and H_2S production as a function of reduction temperature. To facilitate the description, TPR profiles can be divided into two regions: region I, 50–400°C; region II, 400–700°C. The results are presented in Table 4.

On all catalysts, the comparison between H_2 consumption and H_2S desorption profiles of the sulfided Mo catalysts indicates that two distinct species (about 200°C and about 500°C) of Mo are present on the catalysts. They are sulfided ones because one H_2 consumption peak corresponds to one H_2S desorption peak.

A third species is observed on the TPR-H_2 profiles at 900°C and characterized only by H_2 consumption with no H_2S production. This peak can be attributed to residual oxide species (MoO_3). These were observed for Mo/HY catalysts at high Mo loading (5.1%, 8.3%) and their quantities increase with increasing Mo content. These results are in agreement with the decrease of the sulfidation degree reported in Table 1 for the different Mo/HY catalysts and also with the TEM analysis.

The H_2 consumption profiles are very different on the sulfided Mo/HY catalysts and on the Mo/Al_2O_3 catalyst. The first species presenting a high quantity on the alumina supported catalyst (maximum at 220°C) is usually attributed to the active Mo sites on the edge and corner sites of MoS_2 slabs [37]. This species is present in very less amounts on the HY supported catalysts. The distribution of Mo species on alumina and on HY zeolite is therefore very different.

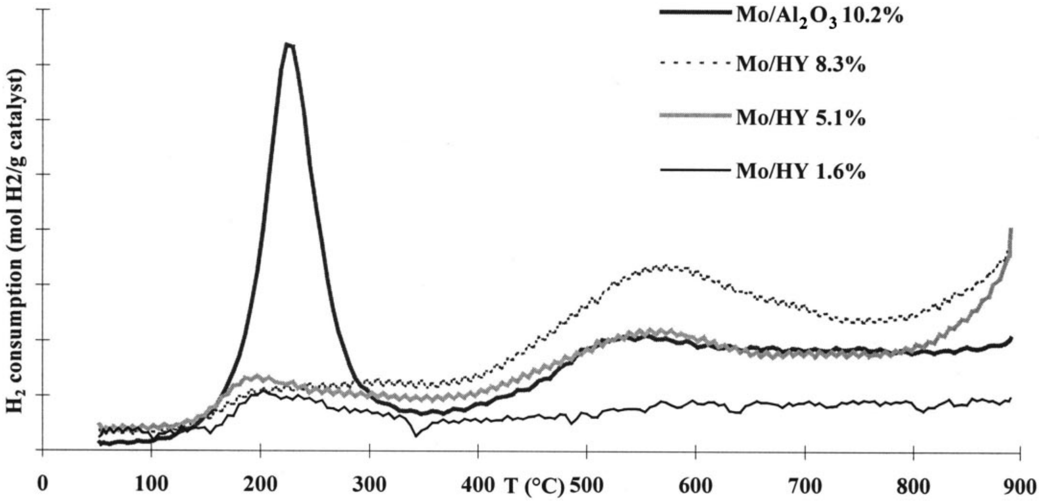

Fig. 4. TPR H_2 consumption profiles of sulfided Mo catalysts.

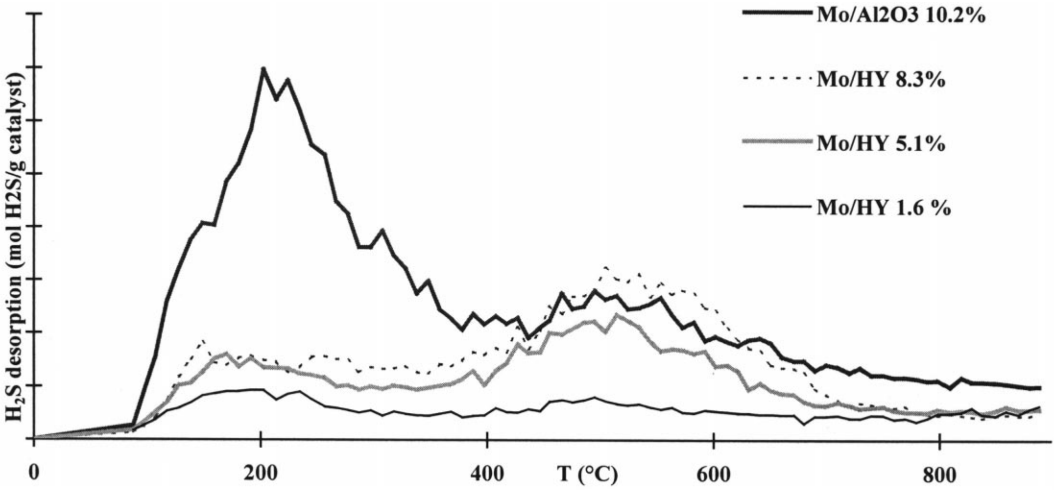

Fig. 5. TPR H_2S desorption profiles of sulfided Mo catalysts.

Moreover, the H_2 consumption per Mo atom indicates that on the HY zeolite and especially at low Mo loading, the Mo species are much more reducible than on alumina (about 0.86 mol H_2/mol Mo on HY zeolite against about 0.38 mol H_2/mol Mo on alumina). Simultaneously, the quantity of H_2S produced during TPR is also higher for the zeolite supported catalysts (1.59 mol H_2S/mol Mo at low Mo content on HY zeolite against 0.50 mol H_2S/mol Mo on alumina).

Obviously, distinct “reducible and sulfurable species” were present on HY zeolite (especially at low Mo contents) that do not exist on alumina. These species could be attributed to the small aggregates observed by TEM and STEM-EDX analysis and MoS_x clusters detected by EXAFS experiments.

We can suppose that this kind of sulfided Mo cluster species would be responsible for the major part of the catalytic activity of the Mo/HY catalysts in toluene hydrogenation. Indeed, these sulfided clusters are much more active than the MoS_2 slab-like species supported on HY that appear at higher Mo content or the conventional MoS_2 slabs of alumina supported catalysts.

The TEM results show the homogeneous distribution of molybdenum sulfide particles in the zeolite framework. It is also possible that the acidity of the zeolite promotes the hydrogenation activity of these small sulfided particles.

The catalytic results exhibit only little change as a function of Mo content for the HY supported catalysts. This can be an indirect evidence for the low effect of HY acidity on the hydrogenation activity of the MoS_2 slabs. An important effect of the acidity of zeolite on the hydrogenation activity of MoS_2 slabs is that, at higher Mo loading (5.1 and 8.3%) the activity of the Mo/HY catalysts should increase significantly.

Table 4
H_2 consumption and H_2S desorption during TPR

Catalysts	Mo loading (wt.%)	H_2 consumption region I + region II		H_2S desorption region I + region II	
		μmol H_2/g_{cata}	mol H_2/mol Mo	μmol H_2S/g_{cata}	mol H_2S/mol Mo[a]
Mo/HY	1.6	147	0.86	330	1.59
Mo/HY	5.1	346	0.65	579	1.00
Mo/HY	8.3	415	0.48	706	0.77
Mo/Al_2O_3	10.1	397	0.38	1155	0.50

[a] H_2S desorption values of the catalysts were corrected by the amounts of H_2S adsorbed on pure support (61 μmol H_2S/g for HY and 776 μmol H_2S/g for Al_2O_3).

It is possible that the MoS_x clusters are highly active only in the proximity of an acidic site, and the extremely high intrinsic activity of these species indicates their presence inside HY cages.

4. Conclusions

Mo/HY catalysts are highly active in toluene hydrogenation under typical hydrotreating conditions. The intrinsic activity of low loading Mo/HY catalysts is far higher than those of standard $NiMo/Al_2O_3$ and $CoMo/Al_2O_3$ catalysts. This high activity can be attributed to small molybdenum sulfide clusters inside the zeolite which are more active than MoS_2 slabs. Their high activity could be both due to their intrinsic activity and their proximity to acid sites.

References

[1] A. Stanislaus, B.H. Cooper, Catal. Rev. Sci. Eng. 36 (1994) 75.
[2] H. van Bekkum, E.M. Flanigen, J.C. Jansen (Eds.), Introduction to Zeolite Science and Practice, Elsevier, Amsterdam, 1991.
[3] W.J.J. Welters, V.H.J. de Beer, R.A. van Santen, Appl. Catal. 119 (1994) 253.
[4] M. Laniecki, W. Zmierczak, Zeolites 11 (1991) 18.
[5] J. Léglise, J.M. Manoli, C. Potvin, G. Djega Mariadassou, D. Cornet, J. Catal. 152 (1995) 275.
[6] P.L. Arias, J.F. Cambra, M.B. Guemez, J.A. Legaretta, B. Pawelec, J.L.G. Fierro, B. Soc. Chim. Belg. 104 (1995) 197.
[7] M. Breysse, M. Cattenot, V. Kougionas, J.C. Lavalley, F. Maugé, J.L. Portefaix, J.L. Zotin, J. Catal. 168 (1997) 143.
[8] R. Cid, J.L.G. Fierro, A. Lopez Agudo, Zeolites 10 (1990) 95.
[9] W.J.J. Welters, Ph.D. Thesis, Eindhoven University of Technology, The Netherlands, 1994.
[10] W.M.H. Sachtler, A.Y. Stakheev, Catal. Today 12 (1992) 283.
[11] Y. Okamoto, A. Meazawa, H. Kane, T. Imanaka, in: M.J. Phillips, M. Ternan (Eds.), Proceedings of the Ninth International Congress on Catalysis, Chemical Institute of Canada, Calgary, June 1988, Ottawa, Vol. 1, 1988, p. 11.
[12] Y. Okamoto, A. Meazawa, H. Kane, T. Imanaka, J. Mol. Catal. 52 (1989) 337.
[13] Y. Okamoto, Stud. Surf. Sci. Catal. 100 (1996) 77.
[14] H. Minning, R.F. Howe, J. Catal. 108 (1987) 283.
[15] A. Lopez Agudo, R. Cid, F. Orellana, J.L.G. Fierro, Polyhedron 5 (1987) 187.
[16] R. Cid, F.J. Llambias, J.L.G. Fierro, A. Lopez Agudo, J. Villasenor, J. Catal. 89 (1987) 478.
[17] J. Léglise, A. Janin, J.C. Lavalley, D. Cornet, J. Catal. 114 (1988) 388.
[18] A. Ezzamarty, E. Catherine, D. Cornet, J.F. Hemidy, J.F. Janin, J.C. Lavalley, J. Léglise, Stud. Surf. Sci. Catal. 49 (1989) 1025.
[19] T.I. Koranyi, L.J.M. van de Ven, W.J.J. Welters, J.W. de Haan, V.H.J. de Beer, R.A. van Santen, Catal. Lett. 17 (1993) 105.
[20] J.A. Anderson, B. Pawelec, J.L.G. Fierro, Appl. Catal. 99 (1993) 37.
[21] A.V. Kucherov, A.A. Slinkin, Zeolites 7 (1987) 38.
[22] J. Thoret, C. Marchal, C. Doremieux-Morin, P.P. Man, M. Gruia, J. Fraissard, Zeolites 13 (1993) 269.
[23] F.L.G. Fierro, J.C. Conesa, A. Lopez Agudo, J. Catal. 108 (1987) 334.
[24] A. Michalowicz, Ph.D. Thesis, Paris-Val de Marne, France, 1990.
[25] R. Cid, F.J. Gil Llambias, M. Gonzales, A. Lopez Agudo, Catal. Lett. 24 (1994) 147.
[26] A. Lopez Agudo, A. Benitez, J.L.G. Fierro, J.M. Palacios, J. Neira, R. Cid, J. Chem. Soc. Faraday Trans. 88 (1992) 385.
[27] G. Vorbeck, W.J.J. Welters, L.J.M. van de Ven, H.W. Zandbergen, J.W. de Haan, V.H.J. de Beer, R.A. van Santen, Stud. Surf. Sci. Catal. 84 (1994) 1617.
[28] W.J.J. Welters, G. Vorbeck, H.W. Zandbergen, L.J.M. van de Ven, E.M. van Oers, J.W. de Haan, V.H.J. de Beer, R.A. van Santen, J. Catal. 161 (1996) 819.
[29] J.A. Anderson, B. Pawelec, J.L.G. Fierro, P.L. Arias, F. Duque, J.F. Cambra, Appl. Catal. 99 (1993) 55.
[30] Y. Feldman, G.L. Frey, M. Homyonfer, V. Lyakhovitskaya, L. Margulis, H. Cohen, G. Hodes, J.L. Hutchison, R. Tenne, J. Am. Chem. Soc. 118 (1996) 5362.
[31] Y. Feldman, V. Lyakhovitskaya, R. Tenne, J. Am. Chem. Soc. 120 (1998) 4176.
[32] R.G. Dickinson, L. Pauling, J. Am. Chem. Soc. 45 (1923) 1466.
[33] M. de Boer, A.J. van Dillen, D.C. Koningsberger, J.W. Geus, J. Phys. Chem. 98 (1994) 7862.
[34] C. Calais, N. Matsubayashi, C. Geantet, Y. Yoshimura, N. Shimada, A. Nishijima, M. Lacroix, M. Breysse, J. Catal. 174 (1998) 130.
[35] T. Shido, R. Prins, J. Phys. Chem. 102 (1998) 8426.
[36] E. Diemann, A. Müller, P.J. Aymonin, Z. Anorg. Allg. Chem. 479 (1981) 191.
[37] M. Salmeron, G.A. Somorjai, A. Wold, R.R. Chianelli, K.S. Liang, Chem. Phys. Lett. 90 (1982) 105.